X-ray absorption study of the $(Y_{1-x}Pr_x)Ba_2Cu_3O_{7-\delta}$ system

1999 J. Phys.: Condens. Matter 11 1847

(http://iopscience.iop.org/0953-8984/11/7/014)

J. Phys.: Condens. Matter **11** (1999) 1847–1859. Printed in the UK PII: S0953-8984(99)94346-1

X-ray absorption study of the $(Y_{1-x}Pr_x)Ba_2Cu_3O_{7-\delta}$ system

S J Gurman†, J C Amiss‡, M Khaled§, N L Saini§ and K B Garg§

† Department of Physics and Astronomy, University of Leicester, Leicester LE1 7RH, UK and CLRC Daresbury Laboratory, Warrington WA4 4AD, UK
‡ BMS, Sheffield Hallam University, Sheffield S1 1WB, UK
§ Department of Physics, University of Rajasthan, Jaipur 302004, India

Received 14 May 1998, in final form 1 November 1998

Abstract. X-ray absorption spectroscopy has been used to investigate the environment of all four cations in a series of six samples of $Y_{1-x}Pr_xBa_2Cu_3O_{7-\delta}$ ($x = 0.0$, 0.2, 0.4, 0.6, 0.8 and 1.0). Interatomic distances and their mean square variations, together with some coordination numbers, have been obtained from an analysis of the EXAFS using the multiple-scattering fast curved-wave theory. The environments of the Ba, Cu and Y atoms were found to be invariant with changing composition, the structural parameters being in good agreement with crystallographic data for the end-point materials. The environment of the Pr atom *was* found to change with composition, both the mean Pr–O distance and its mean square variation varying in a characteristic way. The variations with composition may be closely modelled by the forms $R_{Pr-O} = (2.39 + 0.16x)$ Å and $\sigma^2_{Pr-O} = (40 + 350x(1 - x)) \times 10^{-4}$ Å^2. These results have been interpreted in terms of a combination of *two* Pr–O distances, each invariant with composition, the proportions of these varying linearly with praseodymium content. The consequences of this variation, both for the praseodymium valence and the superconducting properties of the material, are considered.

1. Introduction

Since the discovery in 1986 of superconductors with transition temperatures above 77 K much effort has been devoted to understanding the origin and mechanism of high T_c superconductivity and in a search for new high T_c materials. Investigation of the effects of changes in the structure and electron density of the material on the superconducting transition temperature hold the promise of furthering our understanding of the origin of superconductivity in oxide superconductors. Much of this work results in the production of extremely complex materials since it involves partial replacement of one chemical constituent of the basic material with another. X-ray spectroscopy, in particular extended x-ray absorption fine structure (EXAFS) studies, is an ideal technique for investigating the structure of such complex materials. By measuring and analysing the structure on the absorption edges of all the cations, and in some cases also the oxygen atoms, present in the material the local environment of each can be independently determined and a picture of the structure, including local distortions, built up.

The classic high T_c material $YBa_2Cu_3O_{7-\delta}$ (Y123), whose unit cell is shown in figure 1, has a transition temperature T_c of about 92 K. Replacement of the yttrium by almost all rare earth elements results in a structurally similar material with essentially the same transition temperature. The exceptions are cerium, which only gives multi-phase

0953-8984/99/071847+13$19.50

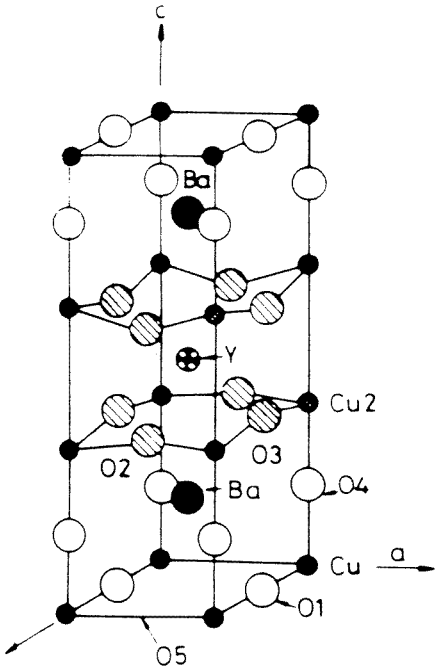

Figure 1. Unit cell of $YBa_2Cu_3O_7$.

materials, and praseodymium. Substitution of Pr for Y, to give $Y_{1-x}Pr_xBa_2Cu_3O_{7-\delta}$, results in single phase materials with the same structure as Y123. However, the transition temperature falls, roughly linearly with Pr content, and the material is not superconducting for $x > 0.55$. In the normal state, a metal–insulator transition occurs at about the same composition.

The general view is that the critical temperature is depressed in $Y_{1-x}Pr_xBa_2Cu_3O_{7-\delta}$ due to a decrease in the concentration of mobile holes. Fehrenbacher and Rice [1] calculated the electronic structure of Pr123 and showed that the absence of superconductivity in this material is due to the existence of a local Pr 4f–O 2p hybridized state which binds holes to the Pr site. The strength of this hybridization will depend on the Pr–O distance. The observation that T_c depends on the mean rare-earth ionic radius in many mixed cuprate materials [2] supports this idea. A change in Pr–O distance may be expected to change the Pr valence and several measurements [3, 4] show such a change. However, some x-ray spectroscopy and photoemission measurements [5, 6] suggest that Pr occurs only in the trivalent state in these materials, although others [7, 8], including our XANES results [9], do suggest a variable Pr valence. Such results may, however, be affected by the perturbing effects of the holes introduced.

We here report the results of an EXAFS study of all four cation edges in a series of samples of $Y_{1-x}Pr_xBa_2Cu_3O_{7-\delta}$ with $x = 0.0$, 0.2, 0.4, 0.6, 0.8 and 1.0. This study provides detailed structural information, in particular on local distortions around the Y and Pr sites. We also briefly consider the XANES results [9] which indicate possible valence changes. Our results are interpreted in terms of a change in the valence of the Pr ion, from 4+ close to $x = 0$ to 3+ at $x = 1.0$.

2. Sample, experimental and data analysis details

2.1. Sample preparation and characterization

Samples of $Y_{1-x}Pr_xBa_2Cu_3O_{7-\delta}$ ($x = 0.0$, 0.2, 0.4, 0.6, 0.8 and 1.0) were prepared from mixtures of the pure oxides by the standard solid state reaction method. The furnace was microprocessor controlled to give very stable preparation conditions. The x-ray diffraction patterns obtained from the samples showed them to be single phase with an orthorhombic structure throughout the composition range.

DC resistivity measurements showed the samples to be metallic in the normal state for $x < 0.6$ and semiconducting for higher Pr content. The transition temperature fell monotonically from $x = 0$ ($T_c = 89$ K ($x = 0.0$), 58 K (0.2) and 32 K (0.4)), the samples being non-superconducting for $x = 0.6$.

2.2. X-ray spectroscopy

X-ray absorption spectra were measured for all four cation species in our samples using the 2 GeV synchrotron source at the CLRC Daresbury Laboratory, UK. The edges used for both EXAFS and XANES studies were the Ba L_3 edge (5247 eV), the Pr L_2 edge (6440 eV—the Pr L_3 edge is obscured by the overlapping Ba L_1 edge), the Cu K edge (8979 eV) and the Y K edge (17 038 eV). Data were also taken for the Pr L_3 edge over a short energy range for XANES studies. All data were obtained in transmission mode at room temperature, using samples with a total absorption–thickness product $\mu t \sim 2$. These were prepared by finely grinding the samples, mixing them with an appropriate quantity of boron nitride and mounting them under light pressure in thin cardboard holders fitted with Sellotape windows. Beam currents during data taking were generally about 200 mA. Beam intensities before (I_0) and after (I_t) transmission through the sample were measured using ion chambers filled with an Ar/He gas mixture, the gas composition being set to give 20% (I_0) or 80% (I_t) absorption at a total gas pressure of 1000 mbar. Three or four spectra, each taking about 30 min to obtain, were averaged to give the final data.

The yttrium K edge data were obtained using station 9.2. This is equipped with a water-cooled, harmonic-rejecting, double-crystal Si(220) monochromator. Harmonic rejection was achieved using a 50% detune from the Bragg peak. An energy range corresponding to photoelectron wavevectors k of 0–15 $Å^{-1}$ was used above the edge.

The barium L_3, praseodymium L_2 and copper K edges were measured using station 7.1. This has a harmonic-rejecting double-crystal Si(111) monochromator. Again harmonic rejection was achieved using a 50% detune. The energy range used for the copper K edge corresponded to $k = 0$–15 $Å^{-1}$ whilst those used for the barium and praseodymium L edges were limited to $k = 0$–10 $Å^{-1}$ by the presence of higher-energy L edges.

In all cases data were taken with a 10 eV step over a long pre-edge region, a 0.5 eV step over the edge and then at a constant k step of 0.05 $Å^{-1}$ in the EXAFS region. In this last case, the counting time per point was scaled by k to maximize counting efficiency. This is particularly important in the case of the Pr L_2 edge which appears as a rather weak edge step on the strong background Ba absorption.

2.3. EXAFS data analysis

The software on both stations 7.1 and 9.2 produces as output counts which are proportional to the beam intensity before and after transmission through the sample as functions of the monochromator angle. This data was converted to a measure of absorption $\ln(I_t/I_0)$ and

calibrated in terms of the photon energy using the standard Daresbury program EXCALIB [10]. This program was also used to sum the spectra obtained from each sample.

The measured absorption spectra were background subtracted and normalized using the standard Daresbury program EXBACK [10]. This fits low-order polynomials to both the pre- and post-edge regions to represent the contribution of other absorption edges and the smooth atomic absorption respectively. These were then subtracted from the data in the usual way to obtain the EXAFS function as a function of photon energy. This program was also used to obtain normalized K or L edge absorption spectra for the XANES studies. The spectra for this purpose had the pre-edge absorption subtracted: the remaining spectrum was then normalized to unit intensity at a standard energy some 50 eV above the edge.

Structural information on the samples was obtained by multi-parameter fitting of the experimental EXAFS data using the EXCURV92 package [10]. Fitting was carried out in k space, i.e. on the unfiltered EXAFS data. This program uses the rapid curved-wave theory of Gurman *et al* [11]. In general, only single-scattering contributions were included. However, the program includes a facility for including multiple scattering up to third order [12]. Multiple-scattering contributions are significant when atoms are, or are nearly, in line. In the present case this occurs only for the Cu–O–Cu coordinations and multiple-scattering contributions were included for these.

For successful application of the theory it is necessary to have a reliable set of electron-scattering parameters. The scattering phase shifts used were calculated for each atom type within EXCURV92 using complex, energy-dependent potentials obtained using the Hedin–Lundqvist theory. Such potentials include, albeit approximately, the effects usually described by the electron mean free path and amplitude reduction factors.

EXCURV92 uses a non-linear, least squares fitting procedure to match the results of the fast curved-wave theory to the experimental EXAFS data. The structure is described in terms of *shells* of atoms, a shell being a set of atoms of identical chemical type and with identical structural parameters. The structural parameters involved are the interatomic distances R_i and the energy offset EF, which together control the phase of the EXAFS and the coordination numbers N_i and mean square variations in R_i, σ_i^2: these fix the amplitude of the EXAFS. The last-named parameter is often referred to in EXAFS studies as the Debye–Waller factor.

The program varies selected parameters until a minimum is obtained in the fit index FI. The fit index used is defined by

$$\mathrm{FI}(\%) = \frac{100}{N_p}\sum_{1}^{N_p}\left\{\frac{[\chi_i(\mathrm{calc}) - \chi_i(\mathrm{exp})]}{\chi_i(\mathrm{exp})}k^n\right\}^2$$

where N_p is the number of data points and n is a k-weighting factor which is used to approximately equalize the contribution of all data points to FI. $n = 3$ was used throughout this work.

A non-trivial problem encountered when using this type of curve-fitting approach is the estimation of the uncertainties in the fitted parameters. This problem is complicated by the presence of correlation between the parameters, especially the pairs (EF, R_i) and (N_i, σ_i^2), which is introduced by the finite extent of the available data. We have used the statistical tests described by Joyner *et al* [13] to estimate these uncertainties. These tests, which form an integral part of EXCURV92, provide a plot of the 95% significance region ($\pm 2\sigma$ uncertainty) on a contour map of FI when this is plotted as a function of two correlated variables and a set of 1σ uncertainties, obtained from the correlation matrix, when more than two variables are varied simultaneously. We always quote 2σ uncertainties in the tables of structural parameters which we give here. The tests may also be used to determine whether a particular shell of atoms gives a significant contribution to the fit. Unless otherwise stated, all of the

shells whose parameters are given here improve the fit significantly at the 95% confidence level.

3. EXAFS results

Our fits to the EXAFS spectra from the four cation edges in $Y_{1-x}Pr_xBa_2Cu_3O_{7-\delta}$ were guided by the diffraction results (as the diffraction data fitting is guided by the chemistry) for the endpoint materials since EXAFS does not contain enough information for a completely *ab-initio* fit. Thus, with the exception of the nearest-neighbour oxygen shells, the coordination numbers were held fixed at values corresponding to high-symmetry crystal sites (see figure 1). We also omitted some weak shells. Thus no oxygen coordinations other than the nearest neighbours are included and cation–cation shells with $N = 1$ were left out of the fits.

The presence of data for all cations means that the results have internal consistency checks: thus the Y–Cu parameters must be consistent with the Cu–Y parameters. We did not impose these constraints during fitting (except for the coordination number constraint mentioned) but use them as a check on the structural parameters after fitting each edge separately. The consistency of our results is considered in detail below.

We found no evidence, at the EXAFS level of sensitivity (about 10%), for any substitution of yttrium or praseodymium cations onto barium or copper sites or *vice versa*, as has been suggested by Lytle *et al* [7]. The strongest evidence for this is the cation–oxygen distance, supported by the cation–copper distance. Thus we take it that yttrium and praseodymium occupy the cell centre site at (0.5, 0.5, 0.5) only. The data are best fitted under the assumption that Y and Pr occupy this site randomly, although the data are only weakly sensitive to ordering of this occupancy, and this is assumed throughout.

The results of the EXAFS data analysis are summarized in table 1. A typical EXAFS spectrum, and its (phase-corrected) Fourier transform, together with the fits to them, are shown in figure 2. The 2σ uncertainties quoted in table 1 are statistical uncertainties. Systematic errors may also be present, due to deficiencies in the EXAFS theory and in the calculated scattering parameters. We assess these by use of the consistency conditions mentioned above and by comparison with diffraction data for the end-point materials. Such systematic errors are considered in sections 3.5 and 4.

3.1. Barium L_3 edge

Because of the presence of the L_2 edge, the barium L_3 edge EXAFS can only be obtained out to $k \sim 9.5$ Å^{-1}. However the edge step is strong and the signal to noise ratio good.

Taking the Ba–O coordination as a single shell gave good fits, with a composition-independent distance of 2.79 ± 0.02 Å, a coordination number always consistent with 12 and a large value of the mean square variation in distance of $(160 \pm 40) \times 10^{-4}$ Å^2. The crystal structure suggests that about 60×10^{-4} Å^2 of this is a static variation, arising from the three different contributions to this shell. This still leaves a rather large thermal contribution of $(100 \pm 40) \times 10^{-4}$ Å^2, implying rather weak Ba–O bonding. Fits could be obtained with this shell split into three components, each containing four oxygen atoms, but the improvement in fit index was rarely significant, due to the short data range. The three distances were found to be 2.70, 2.80 and 2.95 Å, all ± 0.05 Å, each having a mean square variation of $(80 \pm 40) \times 10^{-4}$ Å^2, in line with the estimate given above.

The second shell Ba–Cu coordination was fitted at a composition-independent distance of 3.45 ± 0.02 Å. This is an average of two slightly different distances according to the crystallography. The coordination number is poorly defined, but always consistent with eight, and the mean square variation in distance $(100 \pm 30) \times 10^{-4}$ Å^2.

Table 1. EXAFS results for $Y_{1-x}Pr_xBa_2Cu_3O_{7-\delta}$. Where a formula appears in a table entry, the parameter was found to vary with composition in that manner. The uncertainties on the distance determinations are ±0.02 Å unless otherwise stated. Coordination numbers without uncertainties were held fixed. Uncertainties quoted are 95% confidence limits ($\pm 2\sigma$).

Coordination	Number	Distance (Å)	Mean square variation (10^{-4} Å^2)
Barium L_3 edge			
Ba–O	11.5 ± 1.5	2.79	160 ± 40
Ba–Cu	8	3.45	100 ± 30
Ba–Ba	4	3.83 ±0.02	90 ± 20
Copper K edge			
Cu–O	0.7	1.80 ± 0.05	40 ± 40
Cu–O	3.6 ± 0.5	$1.91 + 0.03x$	40 ± 20
Cu–O	0.7	2.3 ± 0.1	40 ± 40
Cu–Y/Pr	2.7	3.15 ± 0.05	90 ± 50
Cu–Ba	5.3	3.38 ± 0.05	140 ± 60
Cu–Cu	4	3.90 ± 0.05 ±0.02	60 ± 20
Cu–O–Cu (mean)	$155 \pm 5^\circ$		
The Cu–Y/Pr occupancy was assumed to be random.			
Praseodymium L_2 edge			
Pr–O	8 ± 1	$2.39 + 0.16x$	$[40 + 350x(1-x)] \pm 20$
Pr–Cu	8	3.28 ± 0.05	70 ± 20
Pr–Pr	$4x$	3.92	80 ± 60
Pr–Y	$4(1-x)$	3.83 ± 0.05 ±0.02	70 ± 50
The Pr–Pr/Y occupancy was assumed to be random.			
Yttrium K edge			
Y–O	8 ± 1	2.36	65 ± 20
Y–Cu	8	3.22	65 ± 15
Y–Ba	2	3.68	40 ± 20
Y–Y	$4(1-x)$	3.90 ± 0.05	60 ± 20
Y–Pr	$4x$	3.90 ± 0.05 ±0.02	60 ± 20
Y–Y and Y–Pr fourth coordination: random occupancy of site assumed.			

The third shell Ba–Ba coordination corresponds to the edge of the base plane. A composition-independent distance of 3.83 ± 0.02 Å was found. Taking the coordination number as four gave a mean square variation of $(90 \pm 20) \times 10^{-4}$ Å^2.

3.2. Copper K edge

The copper environment in 123 semiconductors is complex due to the presence of two different copper sites, CuI and CuII (see figure 1). This leads to many interatomic distances, some of them of very low mean coordination. We have omitted these where they are overlapped by other strong shells. In addition, we have to consider the possibility of multiple-scattering contributions for the linear (CuI) or nearly linear (CuII) Cu–O–Cu coordinations along the cube edges.

Good data were obtained out to $k = 14$ Å^{-1} on the copper K edges of all samples. The EXAFS corresponds to the sum of contributions from one CuI and two CuII atoms.

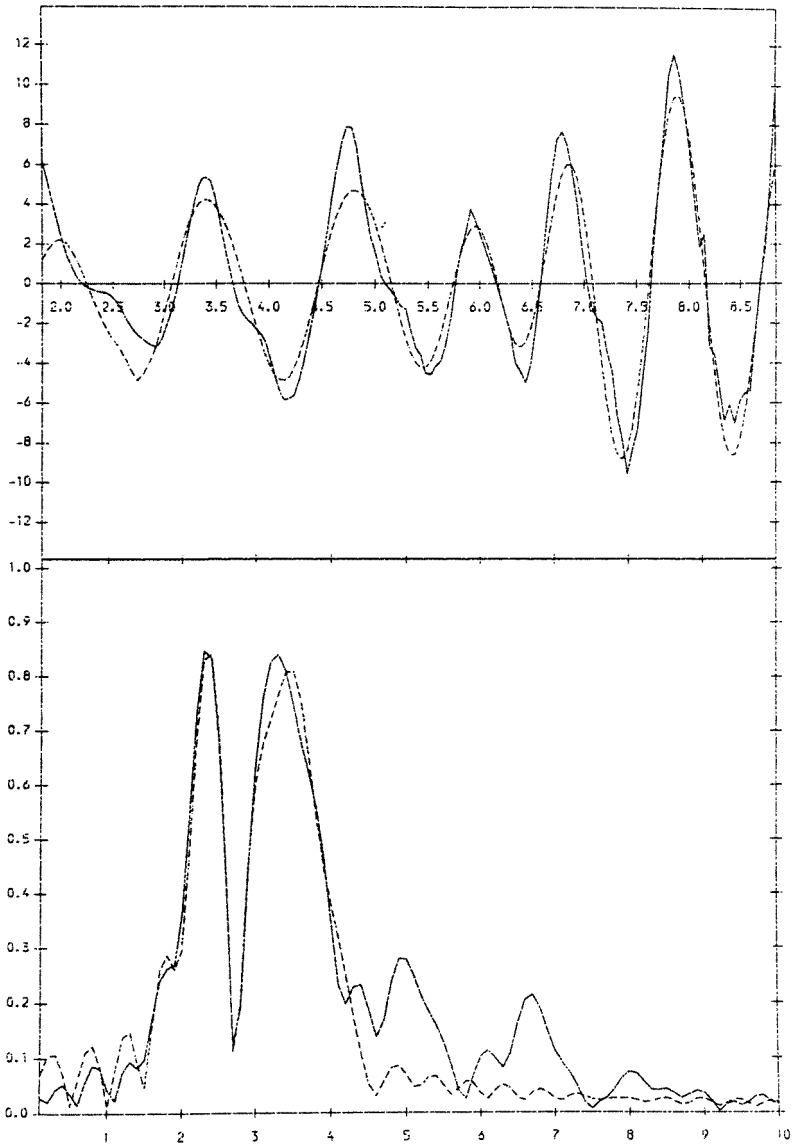

Figure 2. k^3-weighted EXAFS and its phase-corrected Fourier transform from the Pr L_2 edge from the sample with $x = 0.6$. Solid line: experiment; dashed line: theory.

The crystallography gives three Cu–O coordinations, with mean occupancies of 0.7, 4 and 0.7. The main contribution, with a coordination number always consistent with four, was found at a distance of $(1.91 + 0.03x) \pm 0.02$ Å with the very small mean square variation of $(40 \pm 20) \times 10^{-4}$ Å^2. This contribution is due to both CuI and CuII atoms and is expected to be slightly longer than half the cube edge due to the non-linear nature of the CuII–O–CuII bonds. The crystallography also gives two apical Cu–O oxygen coordinations, a short one (CuI) at 1.8 Å and a long one (CuII) at between 2.2 and 2.4 Å. We could fit both of these weak shells, with fixed coordination numbers, obtaining distances of 1.80 ± 0.05 and 2.4 ± 0.1 Å with mean square variations of $(40 \pm 40) \times 10^{-4}$ Å^2.

The Cu–Pr/Y shell gives a rather weak contribution to the EXAFS and is also mixed. It occurs for CuII only. The fit indices suggest a random occupancy of the Pr/Y site, both central cations lying 3.15 ± 0.05 Å from CuII. With fixed coordination numbers obtained from random site occupancy we find equal mean square variations of $(90 \pm 50) \times 10^{-4}$ Å^2.

The strong Cu–Ba shell was fitted at 3.38 ± 0.05 Å with a mean square variation (N fixed at 5.3) of $(140 \pm 60) \times 10^{-4}$ Å^2. This shell corresponds to two contributions of equal strength (from CuI and CuII) and the crystallography suggests a static contribution of about 30×10^{-4} Å^2 in this, leaving a rather large thermal contribution of $(110 \pm 60) \times 10^{-4}$ Å^2.

The Cu–Cu fourth shell coordination corresponds to the cube edge. The analysis is complicated by the presence of multiple-scattering contributions from the interposed oxygen atom. These were included to third order in our fit, which also allows us to obtain the mean Cu–O–Cu bond angle. The fitted Cu–Cu distance was 3.90 ± 0.05 Å with a mean square variation of $(60 \pm 20) \times 10^{-4}$ Å^2. The mean Cu–O–Cu bond angle was fitted as $155 \pm 5^\circ$. If we assume that the CuI–O–CuI coordination is linear then, on allowing for the shape of the oxygen forward scattering factor, we find a CuII–O–CuII scattering angle of about 30–40° from this mean value. This corresponds to a bond angle of about 140–150° for CuII–O–CuII or 0.6 Å between the CuII and O planes.

3.3. Praseodymium L_2 edge

Praseodymium edge data were difficult to obtain (the K edge was not accessible to us) since the L_3 edge normally used is overlapped by the barium L_1 edge. Hence we used the weaker L_2 edge for EXAFS studies. Due to the strong absorption by barium, it is impossible to get a large edge step for this edge. Hence noise levels are high, leading to a restricted useful k range of 9 Å^{-1}.

The nearest-neighbour Pr–O distance was found to show a characteristic strong variation with composition (figure 3), being fitted at $(2.39 + 0.16x) \pm 0.02$ Å. The coordination number was always consistent with eight, showing that Pr occupies the central (0.5, 0.5, 0.5) site only. The mean square deviation in distance (figure 3) also shows a characteristic strong variation with distance which can be closely modelled by the form $[40 + 350x(1 - x) \pm 20] \times 10^{-4}$ Å^2. Both of these Pr–O parameters suggest significant distortion in the neighbouring oxygen layers which we consider further in section 4.

A fit with two Pr–O distances was also tried. After fixing the coordination numbers at $8(1 - x)$ and $8x$ for the short and long component respectively, the two distances and their mean square variations were found to be independent of composition. The values found for the two distances were 2.38 ± 0.03 and 2.53 ± 0.04 Å. Both mean square variations were fitted at $(50 \pm 30) \times 10^{-4}$ Å^2. The fit indices for this split-shell fit were essentially identical to those found for the single-shell fit.

The second shell Pr–Cu coordination was found at 3.28 ± 0.02 Å, independent of composition. The coordination number was found always to be consistent with eight and fixing at this value gave a mean square variation of $(70 \pm 20) \times 10^{-4}$ Å^2. There is therefore no evidence of composition dependence or distortion in this coordination.

No reliable fits could be obtained for the weak Pr–Ba third shell.

The fourth shell, corresponding to the cube edge, is mixed at general compositions. At $x = 1$ we find Pr–Pr at 3.92 ± 0.02 Å with a mean square deviation of $(80 \pm 60) \times 10^{-4}$ Å^2. These values are independent of x, within rather wide uncertainties, if we assume the occupancy of the central site to be random. In this case we also find Pr–Y at 3.83 ± 0.05 Å with a very similar mean square variation.

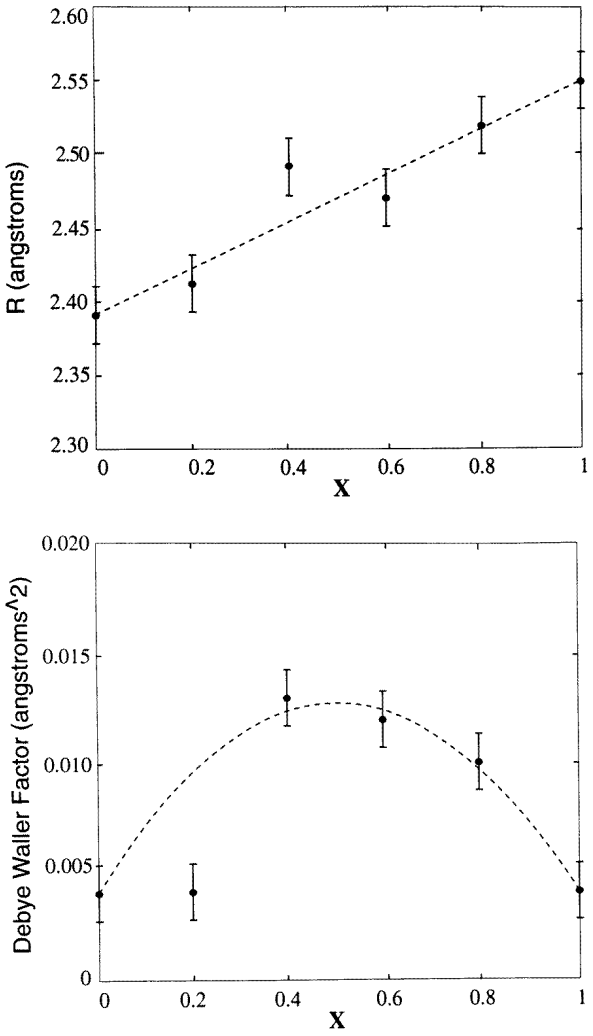

Figure 3. Fitted values of the mean Pr–O distance and its mean square variation as a function of sample composition. The dashed lines represent the simple formulae given in the text.

3.4. Yttrium K edge

Good EXAFS data were obtained for the yttrium K edge out to $k = 15$ Å^{-1}.

The Y–O nearest-neighbour shell was found at 2.36 ± 0.02 Å in all samples. The coordination number was always found to be consistent with eight and with this fixed the mean square variation in distance was $(65 \pm 20) \times 10^{-4}$ Å^2. Thus *no* evidence of distortion or composition dependence was found for this shell.

The Y–Cu second shell was fitted at 3.22 ± 0.02 Å, coordination number always consistent with eight and mean square variation $(65 \pm 15) \times 10^{-4}$ Å^2, all independent of composition.

The Y–Ba third shell, with coordination fixed at two, was found at a distance of 3.68 ± 0.03 Å with a mean square variation of $(40 \pm 20) \times 10^{-4}$ Å^2, again independent of composition.

The fourth shell coordination is mixed Y and Pr at general compositions. For $x = 0.0$ we find Y–Y at 3.85±0.02 Å with $N = 4\pm1$ and a mean square variation of $(90\pm25)\times10^{-4}$ Å^2. If we assume random occupancy of the central site then the parameters are found to be independent of composition. Both the Y–Y and the Y–Pr parameters are then fitted as 3.90 ± 0.05 Å with a mean square deviation of $(60 \pm 20) \times 10^{-4}$ Å^2.

3.5. Consistency

One of the advantages of EXAFS as a structural technique is that data taken from different edges of the same sample provides an internal consistency check which may be used to check for *systematic* errors. The parameters of A–B coordination, the distance, mean square variation and coordination number can be independently determined by analysing the EXAFS from A and B absorption edges. Clearly, the distance and its mean square variation should be the same in the two cases and the coordination numbers are related by $c_A N_{AB} = c_B N_{BA}$, where c_i is an atomic coordination and N_{ij} the number of type j atoms surrounding the type i atom. This last form comes from equating the number of AB coordinations when counted from either end.

Table 2. Consistency between EXAFS fits.

Coordination	Distance (Å)	Mean square variation (10^{-4} Å^2)
Cu–Ba	3.38 ± 0.05	140 ± 60
Ba–Cu	3.45 ± 0.02	120 ± 40
Cu–Y	3.15 ± 0.05	80 ± 40
Y–Cu	3.22 ± 0.02	65 ± 15
Cu–Pr	3.15 ± 0.05	120 ± 50
Pr–Cu	3.25 ± 0.05	70 ± 20

In this work the coordination numbers, where they could be fitted, were always consistent with the crystallographic values, so the last relation holds. We assume such coordination numbers in the majority of cases. Thus we check only the consistency of the distances and their mean square variations. Thus can be done for the three cation pairs Cu–Ba, Cu–Y and Cu-Pr. The results are summarized in table 2.

Cu–Ba. The Ba L_3 edge EXAFS gives Ba–Cu at 3.45 ± 0.02 Å; the Cu K edge EXAFS gives Cu–Ba at 3.38±0.05 Å. There may be some slight biasing of the fits due to the omission of weak shells. The data are consistent and we may set the distance at 3.43±0.03 Å, independent of composition. The mean square variations are $(120\pm40)\times10^{-4}$ Å^2 and $(140\pm60)\times10^{-4}$ Å^2 respectively, in good agreement. About 30×10^{-4} Å^2 of this is static variation due to the two Cu–Ba distances, differing by 0.1 Å according to the crystallography, which we have averaged in our fit.

Cu–Y. The Y K edge data give Y–Cu at 3.22 ± 0.02 Å, the Cu K edge data give Cu–Y at 3.15 ± 0.05 Å, so the two determinations are just consistent. The Cu coordination is mixed (Y + Pr) and, except near $x = 0$, the uncertainties on the Cu–Y distance are large. We therefore put more weight on the Y edge data and fix the Cu–Y distance at 3.22 ± 0.03 Å. The mean square variations are $(65 \pm 15) \times 10^{-4}$ Å^2 and $(80 \pm 40) \times 10^{-4}$ Å^2 respectively, in good agreement.

Cu–Pr. The Pr L_2 edge data give a distance of 3.25±0.05 Å whilst the Cu K edge data give 3.15 ± 0.05 Å. Due to the weakness of the Pr signal, we give these equal weight and set Cu–Pr at 3.20±0.07 Å. The mean square variations are $(70\pm20)\times10^{-4}$ Å^2 and $(120\pm50)\times10^{-4}$ Å^2 again in fairly good agreement.

4. Discussion

Diffraction data are available for the two end-point materials, with $x = 0.0$ or 1.0, and we first compare our results with these. There are variations of up to 0.05 Å between the various diffraction determinations of interatomic distances, and also some variation between determinations of the unit cell dimensions. We use the data of Garbauskas *et al* [14] for Y123 and Moran *et al* [15] for Pr123.

All of the distances from Cu atoms determined by EXAFS differ by less than 0.05 Å from the diffraction data. The differences have both signs, so we claim good agreement with diffraction data for our copper K edge results. The same is true for our results from the barium and yttrium edges. The distances determined using the praseodymium L_2 edge are all a little long, by about 0.05 Å on average. This suggests that our calculation of the Pr central atom phase shift is possibly a little inaccurate.

The interatomic distance for the strong Cu–O coordination shows a dependence on composition. This mean distance is expected to be about 0.01 Å longer than half the cube edge (due to the non-linear CuII–O–CuII bonding). The composition variation agrees with the unit cell parameters of the end-point materials and the roughly linear variation is also consistent with the unit cell parameters given by diffraction studies of the mixed crystal [16, 17]. The cube edge is also given by the A–A (e.g. Cu–Cu) cation fourth-neighbour distance, but the precision of our determination of this distance is such that we can say no more than that all of these are consistent with the unit cell dimensions at all compositions.

Determination of the position of the atoms within the unit cell of the mixed crystals is very poorly defined by the diffraction data, which assume superimposed atoms, although there is an indication of a distortion in the oxygen layer close to the CuII atoms. Various site occupancies have been obtained from diffraction studies [16, 17]. Such detailed information on unit cell composition is best obtained by EXAFS and we now concentrate on the information our results provide for changes in the position of atoms as the composition changes.

We first assume that all atoms occupy the same symmetric positions in the (a, b) plane as they do in the end-point materials, Y123 or Pr123. This assumption is justified by the EXAFS data in that, in general, the coordination numbers (where they can be determined) are independent of composition, as are the mean square variations in interatomic distances. The values of the latter parameter indicate that there is no extra splitting of the shells at intermediate compositions. The exception is the Pr–O nearest-neighbour distance: this is considered in detail below. The cation–cation distances show that the cations occupy the same planes as they do in Y123 or Pr123, at essentially the same distances up the c axis. In particular, the EXAFS data show that the cation sites are *well ordered*, at least 90% of the barium atoms occupying the Ba planes, etc. The Y site is occupied, probably randomly, by yttrium and praseodymium atoms only, to the same level of accuracy. This conclusion agrees with some of the diffraction results [16] but disagrees with others [17].

The Pr–O distance was found to vary linearly with composition as $2.39 + 0.16x$ Å. Its mean square variation was found to vary quadratically as $x(1-x)$ (see table 1). No other mean square variation, in particular that for Y–O, varies with composition. We interpret our results in terms of a mixed occupancy of the $z/c = 0.5$ mirror plane. We take this to be occupied at random by Y or Pr atoms. The Y–O distance, to oxygen atoms in the planes at $z/c = 0.37$ and 0.63 is invariant. The Pr–O data can be modelled by taking *two* Pr–O distances: 2.39 Å if the Pr is adjacent to a Y atom in the direction of the Pr–O bond and 2.55 Å if it is adjacent to a Pr atom in that direction. This model was used for the split Pr–O shell fits described in section 3.3. If the Y and Pr atoms are distributed randomly on the mirror plane this model quantitatively gives both the observed linear variation in mean distance and the quadratic variation in mean

square variation of the Pr–O structural parameters, and the invariance of the Y–O parameters, to within our fitting accuracy. The thermal contribution to the mean square variation is much the same for both the yttrium and praseodymium atoms (see table 1). Such a model gives rise to two positions for the neighbouring oxygen atoms, at $z/c = 0.35$ and 0.38, with a corresponding pair at 0.62 and 0.65. These oxygen atoms are those close to the CuII atom and the distortions introduced into the Cu–O bonding may influence the superconducting behaviour of the material. The effects of this distortion will hardly show up in the Cu–O distances due to trigonometric effects.

Our results for the yttrium edge are essentially the same as those obtained by Booth *et al* [8], who investigated samples with $x = 0.0$, 0.3 and 0.5. These authors also analysed data from the Pr K edge measured on samples with $x = 0.3$, 0.5 and 1.0. They also found two Pr–O distances, at 2.27 and 2.44 Å, both about 0.09 Å shorter than our values. The longer bond is about 0.05 Å shorter than that given by diffraction data for Pr123 [15]. These authors found that the shorter bond was highly disordered ($\sigma^2 = 200 \times 10^{-4}$ Å^2) and, perhaps significantly, also existed in the samples with $x = 1.0$, in disagreement with the diffraction data [15]. Booth *et al* [8] did not investigate any other edges in the mixed compounds, nor do they provide any estimate of uncertainties in the structural parameters.

Combining the results from all four cation edges allows us to produce a reasonably self-consistent set of z/c positions for all of the atoms in the unit cell. These are given in table 3. We estimate that these values are accurate to about ± 0.01. We see that the only significant structural effect of substituting Pr for Y is the distortion of the oxygen layer close to the CuII atoms and a steady linear shift in its mean position from $z/c = 0.38$ at $x = 0.0$ to $z/c = 0.35$ at $z = 1.0$. The distortion and shifting of this oxygen layer *does not* lead to a distortion or shift in the position of the CuII layer, as determined by the Y–Cu and Pr–Cu distances. The two different oxygen positions then give two different CuII–O–CuII bond angles, distributed randomly. One is in line, as seen for CuI, when the oxygen atom lies between two Pr atoms, the other has a bond angle of about 160°, found when the oxygen lies between two Y atoms or a Y and a Pr atom. The proportion of in-line atoms varies as x^2 since they correspond to a long Pr–O bond which only occurs when the oxygen atom lies between two Pr atoms.

Table 3. Positions along c-axis: comparison with diffraction data.

		Diffraction		
	EXAFS	Y123[14]	Pr123[15]	Mixed [16]
Atom	z/c	z/c	z/c	z/c
Cu I	0.00	0.00	0.00	0.00
O	0.00	0.0	0.00	0.00
O	0.16	0.154	0.158	0.16
Ba	0.18	0.185	0.185	0.18
Cu II	0.35	0.356	0.350	0.355
O	0.35/0.38	0.378	0.368	0.36/0.40
Y/Pr	0.50	0.50	0.50	0.50

The variation in the mean Pr–O distance with composition suggests that the mean Pr valence may also change. The difference between the bond lengths, 0.16 Å, corresponds almost exactly to a change of unity in the valence if we use the bond valence model [18] with a total coordination of eight. Since Y^{3+} and Pr^{4+} ions are essentially the same size [19], our results suggest a change in Pr valence from 4+ near $x = 0$, to 3+ at $x = 1$, if we take the longer Pr–O distance to correspond to Pr 3+ and the shorter to Pr 4+. The Pr ions will therefore

suck in more electrons as x increases: this effect will be quadratic in x since both the number and the mean valence of Pr ions, assuming this to be proportional to the mean bond length, vary linearly with x. The presence of two distances at mixed compositions suggests that not too much weight should be put on the simple bond valence model (although most complex oxide materials show the presence of several cation–oxygen distances and the model has been successfully applied to these) but a possible change in Pr valence could again be of significance for the superconductivity. Our Pr L_3 XANES results [9] also suggest a change in the Pr valence as the composition changes, as do those of Lytle *et al* [7].

Our EXAFS results suggest that the suppression of superconductivity in mixed Y–Pr 123 compounds is due to changes in the valence of the Pr atom driven by changes in the mean Pr–O distance. These changes arise from the locking of the Y–O distance at about 2.36 Å. The exact mechanism by which the change in valence changes the superconducting transition temperature cannot be determined from our data.

References

[1] Fehrenbacher F and Rice T M 1993 *Phys. Rev. Lett.* **70** 3471
[2] Vasek P, Svoboda P, Pollert E, Zemanova D, Kufudalis A, Mitros Ch, Gamari-Seale H and Niarchos D 1992 *Physica* C **196** 90
[3] Ghamaty G, Lee B W, Neumeier J J, Nieve G and Maple M B 1991 *Phys. Rev.* B **43** 5430
[4] Cooke D W, Kwok R S, Lichti R L, Adams T R, Boekema C, Davison W K, Kebebe A, Schwegler J, Crow J E and Mihalisin T 1990 *Phys. Rev.* B **41** 4801
[5] Horn S, Cai J, Shaheen S A, Jeon Y, Croft M, Chang C L and den Boer M L 1987 *Phys. Rev.* B **36** 3895
[6] Kang J S, Allen J W, Shen Z X, Ellis W P, Yeh J J, Lee B W, Maple M B, Spicer W E and Landau I 1989 *J. Less-Common Met.* **148** 121
[7] Lytle F W, van der Laan G, Greegor R B, Larson E M, Violet C E and Wong J 1990 *Phys. Rev.* B **41** 8955
[8] Booth C H, Bridges F, Boyce J B, Claeson T, Zhao Z X and Cervantes P 1994 *Phys. Rev.* B **49** 3432
[9] Khaled M, Saini N L, Garg K B and Studer F 1996 *Solid State Commun.* **100** 773
[10] Dent A J and Mosselmans J F W 1995 *An Introduction to EXAFS Data Analysis* (Warrington: CLRC Daresbury Laboratory)
[11] Gurman S J, Binsted N and Ross I 1984 *J. Phys. C: Solid State Phys.* **17** 143
[12] Gurman S J 1988 *J. Phys. C: Solid State Phys.* **21** 3699
[13] Joyner R W, Martin K J and Meehan P 1987 *J. Phys. C: Solid State Phys.* **20** 4005
[14] Garbauskas M F, Arendt R H and Kaspar J S 1987 *Inorg. Chem.* **26** 3191
[15] Moran E, Amador U, Barahona M, Alario-Franco M A, Vegas A and Rodriguez-Carvajal J 1988 *Solid State Commun.* **67** 369
[16] Kinoshita K, Matsuda A, Shibata M, Ishii T, Watanabe T and Yamada T 1988 *Japan. J. Appl. Phys.* **27** 1642
[17] Guo Z, Yamada N, Gondaina K I, Iri T and Kohn K 1994 *Physica* C **220** 41
[18] Brown I D 1991 *Solid State Commun.* **90** 155
[19] Shannon R D 1976 *Acta Crystallogr.* **A32** 751